

SEARCH FOR ANOMALOUS $WW\gamma$ AND WWZ COUPLINGS WITH POLARIZED e -BEAM AT THE LHeC*

I.T. ÇAKIR[†]

Applications and Research Centre for Advanced Studies
Department of Electrical and Electronics Engineering, Faculty of Engineering
Istanbul Aydin University, 34295, Sefakoy, Istanbul, Turkey

O. ÇAKIR[‡]

Department of Physics, Faculty of Sciences, Ankara University
06100, Tandogan, Ankara, Turkey

A. SENOL[§], A.T. TASCI[¶]

Department of Physics, Faculty of Science and Arts, Kastamonu University
37100, Kuzezykent, Kastamonu, Turkey

*(Received July 11, 2014; revised version received September 9, 2014;
final version received September 24, 2014)*

We examine the possibility of constraining the anomalous $WW\gamma$ and WWZ couplings by measuring total cross sections of the $ep \rightarrow \nu_e q\gamma X$ and $ep \rightarrow \nu_e qZX$ processes at the LHeC collider with the electron beam energy $E_e = 60$ GeV and $E_e = 140$ GeV. We consider the cases of unpolarized and polarized electron beams. The difference of the upper and lower bounds on the anomalous couplings, $(\delta\Delta\kappa_\gamma, \delta\lambda_\gamma)$ and $(\delta\Delta\kappa_Z, \delta\lambda_Z)$ are obtained as (0.990, 0.122) and (0.362, 0.012) without electron beam polarization at the beam energy of $E_e = 140$ GeV for an integrated luminosity of $L_{\text{int}} = 100 \text{ fb}^{-1}$, respectively. With the possibility of e -beam polarization, we obtain more improved results as (0.975, 0.118) and (0.285, 0.009) for $(\delta\Delta\kappa_\gamma, \delta\lambda_\gamma)$ and $(\delta\Delta\kappa_Z, \delta\lambda_Z)$, respectively. The results are found to be comparable with the current experimental limits obtained from two-parameter fits to the data collected in the lepton and hadron colliders. It

* Funded by SCOAP³ under Creative Commons License, CC-BY 3.0.

[†] ilkayturkcakir@aydin.edu.tr

[‡] ocakir@science.ankara.edu.tr

[§] asenol@kastamonu.edu.tr

[¶] atasci@kastamonu.edu.tr

is found that the limits on the anomalous couplings $(\Delta\kappa_Z, \lambda_Z)$ through the process $ep \rightarrow \nu_e q ZX$ at the LHeC can further improve the current experimental limits.

DOI:10.5506/APhysPolB.45.1947

PACS numbers: 12.60.Cn, 13.88.+e

1. Introduction

Triple gauge boson interactions are the consequence of the $SU(2) \times U(1)$ gauge symmetry of the Standard Model (SM). A precise determination of the trilinear gauge boson couplings is necessary to test the validity of the SM and the presence of new physics up to a high energy scale. Since the tree-level couplings of the $WW\gamma$ and WWZ vertices are fixed by the SM, any deviations from their SM values would indicate the new physics beyond the SM. The photoproduction of the W and Z bosons through triple gauge boson interactions in the lepton-hadron colliders HERA+LC and in the Large Hadron electron Collider (LHeC) has been studied theoretically in the papers [1] and [2], respectively. An investigation of the potential of the LHeC to probe anomalous $WW\gamma$ coupling has been presented in Ref. [3].

The present bounds on the anomalous $WW\gamma$ and WWZ couplings are provided by the LEP [4], Tevatron [5, 6] and LHC [7, 8] experiments. Recently, the ATLAS [7] and CMS [8] collaborations have established updated constraints on the anomalous $WW\gamma$ and WWZ couplings from the $\gamma W(Z)$ and W^+W^- production processes. The best available constraints on anomalous couplings $\Delta\kappa_\gamma$, λ_γ , $\Delta\kappa_Z$ and λ_Z obtained from one-parameter analysis at different experiments are summarized in Table I.

TABLE I

The available 95% C.L. bounds on anomalous couplings $(\Delta\kappa_\gamma, \lambda_\gamma)$ and $(\Delta\kappa_Z, \lambda_Z)$ from the data at LEP, Tevatron, and LHC experiments. In each case, the parameter listed is varied while the others are fixed to their SM values.

	LEP [4]	CDF [5]	D0 [6]	ATLAS [7]	CMS [8]
$\Delta\kappa_\gamma$	[-0.099, 0.066]	[-0.460, 0.390]	[-0.158, 0.255]	[-0.135, 0.190]	[-0.210, 0.220]
λ_γ	[-0.059, 0.017]	[-0.180, 0.170]	[-0.036, 0.044]	[-0.065, 0.061]	[-0.048, 0.048]
$\Delta\kappa_Z$	[-0.073, 0.050]	[-0.414, 0.470]	[-0.110, 0.131]	[-0.061, 0.093]	[-0.160, 0.157]
λ_Z	[-0.059, 0.017]	[-0.140, 0.150]	[-0.036, 0.044]	[-0.062, 0.065]	[-0.048, 0.048]

The current limits based on one-parameter analysis at 95% C.L. on the $\Delta\kappa_\gamma$ and λ_γ from the ATLAS Collaboration with $W\gamma$ production process data at $\sqrt{s} = 7$ TeV and $L_{\text{int}} = 4.6 \text{ fb}^{-1}$ are $(-0.135, 0.190)$ and $(-0.065, 0.061)$ [7]. Similar limits are $(-0.420, 0.480)$ for $\Delta\kappa_\gamma$ and $(-0.068, 0.062)$ for λ_γ

from two-parameter analysis at 95% C.L. Two-parameter 95% C.L. on anomalous couplings $\Delta\kappa_Z$ and λ_Z are given as $(-0.045, 0.045)$ and $(-0.063, 0.063)$, respectively.

According to the CMS Collaboration, the current limits for one-parameter 95% C.L. are $(-0.210, 0.220)$ and $(-0.048, 0.048)$ for $\Delta\kappa_\gamma$ and λ_γ from $W\gamma$ production process at $\sqrt{s} = 7$ TeV and $L_{\text{int}} = 5 \text{ fb}^{-1}$ [8]. From two-parameter contours, the upper and lower limits for $\Delta\kappa_\gamma$ and λ_γ are $(-0.250, 0.250)$ and $(-0.050, 0.042)$ at the 95% C.L., while one-parameter 95% C.L. on $\Delta\kappa_Z$ and λ_Z are $(-0.160, 0.157)$ and $(-0.048, 0.048)$ from W^+W^- production process at $\sqrt{s} = 7$ TeV. Here, the relation $\Delta\kappa_Z = \Delta g_1^Z - \Delta\kappa_\gamma \tan^2 \theta_W$ is used to extract some of the current limits in the LEP scenario. The results from the ATLAS and CMS experiments based on two-parameter analysis of the anomalous couplings are given in Table II.

TABLE II

The available 95% C.L. two-parameter bounds on anomalous couplings $(\Delta\kappa_\gamma, \lambda_\gamma)$ and $(\Delta\kappa_Z, \lambda_Z)$ from the ATLAS and CMS experiments. The difference of the upper and lower bounds are shown in the last two columns.

	ATLAS [7]	CMS [8]	ATLAS (upper-lower)	CMS (upper-lower)
$\Delta\kappa_\gamma$	[-0.420, 0.480]	[-0.250, 0.250]	0.900	0.500
λ_γ	[-0.068, 0.062]	[-0.050, 0.042]	0.130	0.092
$\Delta\kappa_Z$	[-0.045, 0.045]	[-0.160, 0.180]	0.090	0.340
λ_Z	[-0.063, 0.063]	[-0.055, 0.055]	0.126	0.110

In this study, we examined the $ep \rightarrow \nu_e q \gamma X$ and $ep \rightarrow \nu_e q Z X$ processes with anomalous $WW\gamma$ and WWZ couplings at the high energy electron-proton collider LHeC. This collider is considered to be realised by accelerating electrons 60–140 GeV and colliding them with the 7 TeV protons incoming from the LHC. We take into account the possibility of the electron beam polarization at the LHeC which extends the sensitivity to anomalous triple gauge boson couplings. The anticipated integrated luminosity is taken at the order of 10 and 100 fb^{-1} [9].

2. Anomalous couplings

The $WW\gamma$ and WWZ interaction vertices are described by an effective Lagrangian with the coupling constants $g_{WW\gamma}$ and g_{WWZ} , and dimensionless parameter pairs $(\kappa_\gamma, \lambda_\gamma)$ and (κ_Z, λ_Z) ,

$$\begin{aligned}
\mathcal{L} = & ig_{WW\gamma} \left[g_1^\gamma \left(W_{\mu\nu}^\dagger W^\mu A^\nu - W^{\mu\nu} W_\mu^\dagger A_\nu \right) + \kappa_\gamma W_\mu^\dagger W_\nu A^{\mu\nu} \right. \\
& \left. + \frac{\lambda_\gamma}{m_W^2} W_{\rho\mu}^\dagger W_\nu^\mu A^{\nu\rho} \right] + ig_{WWZ} \left[g_1^Z \left(W_{\mu\nu}^\dagger W^\mu Z^\nu - W^{\mu\nu} W_\mu^\dagger Z_\nu \right) \right. \\
& \left. + \kappa_Z W_\mu^\dagger W_\nu Z^{\mu\nu} + \frac{\lambda_Z}{m_W^2} W_{\rho\mu}^\dagger W_\nu^\mu Z^{\nu\rho} \right], \tag{1}
\end{aligned}$$

where $g_{WW\gamma} = g_e = g \sin \theta_W$ and $g_{WWZ} = g \cos \theta_W$. In general, these vertices involve six C and P conserving couplings [10]. However, the electromagnetic gauge invariance requires that $g_1^\gamma = 1$. The anomalous couplings are defined as $\kappa_V = 1 + \Delta\kappa_V$ where $V = \gamma, Z$ and $g_1^Z = 1 + \Delta g_1^Z$. The $W_{\mu\nu}$, $Z_{\mu\nu}$ and $A_{\mu\nu}$ are the field strength tensors for the W boson, Z boson and photon, respectively.

The one-loop corrections to the $WW\gamma$ and WWZ vertices within the framework of the SM have been studied in [11]. These corrections to the $\Delta\kappa_V$ and λ_V have been found to be of the order of 10^{-2} and 10^{-3} , respectively. The values of the couplings $\kappa_\gamma = \kappa_Z = 1$ and $\lambda_\gamma = \lambda_Z = 0$ correspond to the case of the SM. Since unitarity restricts the $WW\gamma$ and WWZ couplings to their SM values at very high energies, the triple gauge couplings are modified as $\Delta\kappa_V(q^2) = \Delta\kappa_V(0)/(1 + q^2/\Lambda^2)^2$ and $\lambda_V(q^2) = \lambda_V(0)/(1 + q^2/\Lambda^2)^2$, where $V = \gamma, Z$. The q^2 is the square of momentum transfer into the process and Λ is the new physics energy scale. The $\Delta\kappa_V(0)$ and $\lambda_V(0)$ are the values of the anomalous couplings at $q^2 = 0$. We assume the values of the anomalous couplings remain approximate constant in the interested energy scale ($\Lambda^2 > q^2$). We take $\Delta\kappa_V$ and λ_V as free parameters in the considered range and find the bounds on these couplings effectively. For the numerical calculations, we have implemented interactions terms in the CalcHEP [12].

3. Production cross sections

According to the effective Lagrangian, the anomalous vertices for triple gauge interactions $WW\gamma$ and WWZ are presented in the Feynman graphs as shown in Figs. 1 and 2. In order to calculate the cross sections for the process $ep \rightarrow \nu_e q \gamma X$ and $ep \rightarrow \nu_e q Z X$, we apply the transverse momentum cut on photon and jet as $p_T^\gamma > 50$ GeV, $p_T^j > 20$ GeV; missing transverse momentum cut $p_T^\nu > 20$ GeV, pseudorapidity cuts $|\eta_{\gamma,j}| < 3.5$; a cone radius cut between photons and jets $\Delta R_{\gamma,j} > 1.5$. Using these cuts and the parton distribution functions of CTEQ6L [13], the total cross sections of the process $ep \rightarrow \nu \gamma q X$ as a function of anomalous couplings $\Delta\kappa_\gamma$ and λ_γ for $E_e = 60$ GeV (140 GeV) with ($P_e = \pm 0.8$) and without ($P_e = 0$) electron beam

polarization are presented in Figs. 3 and 4 (Figs. 5 and 6), respectively. It is clear from these figures that the polarization ($P_e = -0.8$) enhances the cross sections according to the unpolarized case.

The cross sections depending on anomalous couplings $\Delta\kappa_Z$ and λ_Z of the process $ep \rightarrow \nu Z q X$ for $E_e = 60$ GeV (140 GeV) with ($P_e = \pm 0.8$) and without ($P_e = 0$) electron beam polarization are presented in Figs. 7 and 8 (Figs. 9 and 10), respectively.

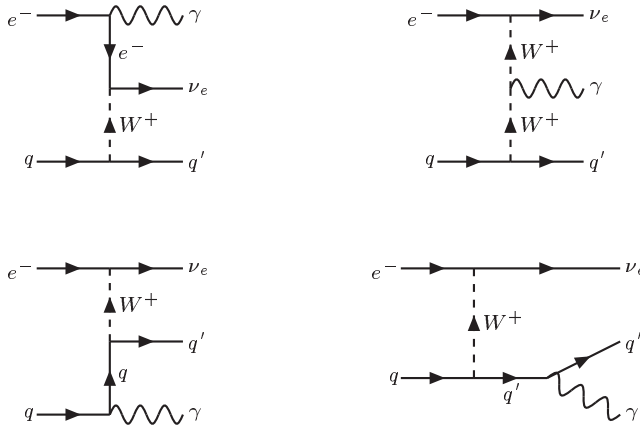


Fig. 1. Representative Feynman diagrams for subprocess $eq \rightarrow \nu_e \gamma q'$.

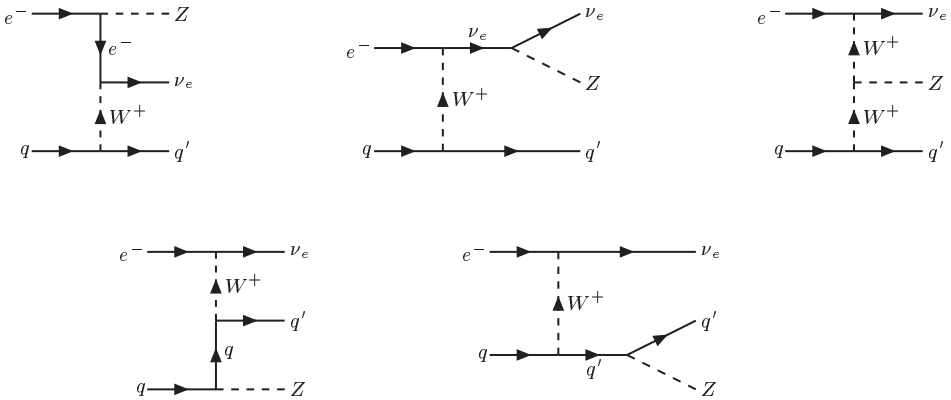


Fig. 2. Representative Feynman diagrams for subprocess $eq \rightarrow \nu_e Z q'$.

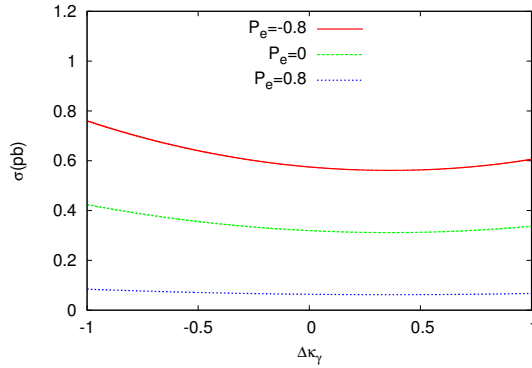


Fig. 3. The cross section depending on anomalous coupling $\Delta\kappa_\gamma$ of the process $ep \rightarrow \nu\gamma qX$ at $E_e = 60$ GeV for different electron beam polarizations.

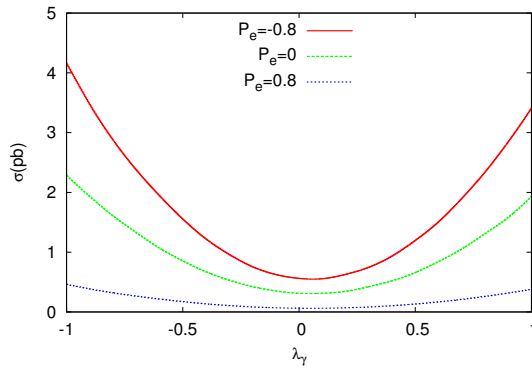


Fig. 4. The cross section depending on anomalous coupling λ_γ of the process $ep \rightarrow \nu\gamma qX$ at $E_e = 60$ GeV for different electron beam polarizations.

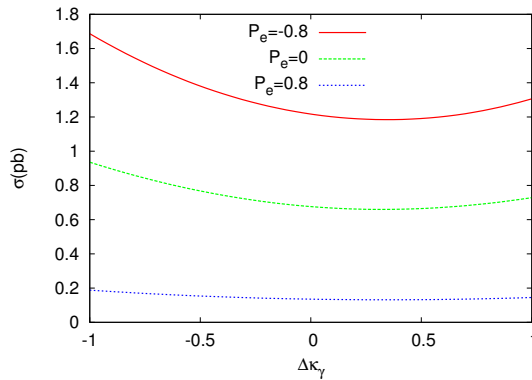


Fig. 5. The same as Fig. 3 but for $E_e = 140$ GeV.

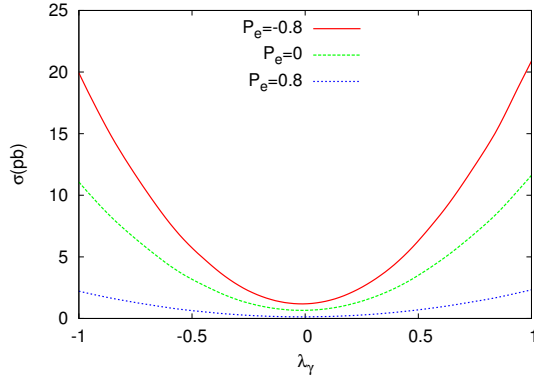


Fig. 6. The same as Fig. 4 but for $E_e = 140$ GeV.

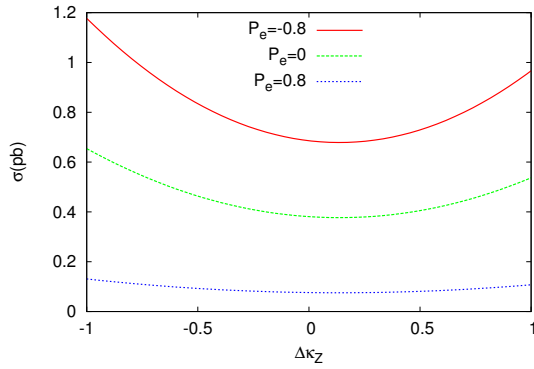


Fig. 7. The cross section depending on anomalous $\Delta\kappa_Z$ coupling of the process $ep \rightarrow \nu Z q X$ for $E_e = 60$ GeV.

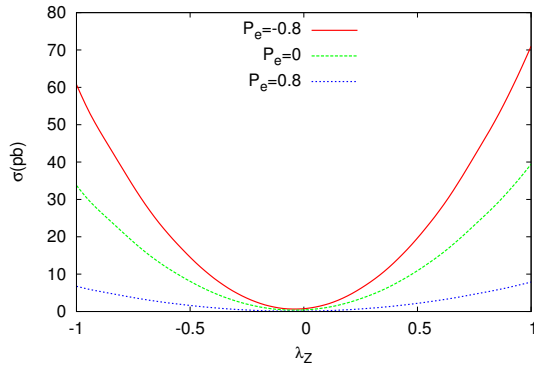


Fig. 8. The cross section depending on anomalous λ_Z coupling of the process $ep \rightarrow \nu Z q X$ for $E_e = 60$ GeV.

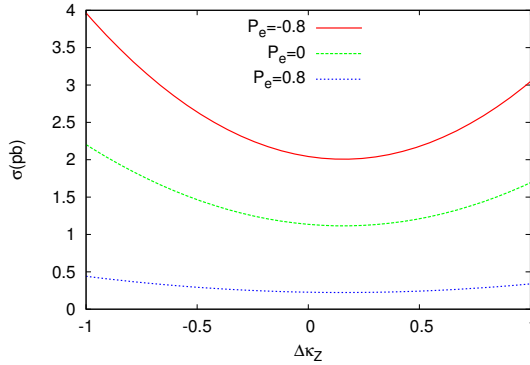


Fig. 9. The same as Fig. 7 but for $E_e = 140$ GeV.

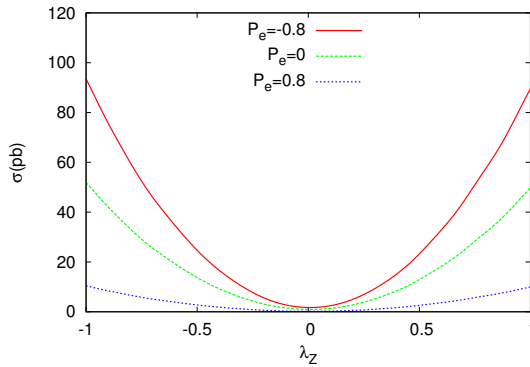


Fig. 10. The same as Fig. 8 but for $E_e = 140$ GeV.

4. Analysis

In order to estimate the sensitivity to the anomalous $WW\gamma$ and WWZ couplings, we use two-parameter χ^2 function

$$\chi^2(\Delta\kappa_V, \lambda_V) = \left(\frac{\sigma_{\text{SM}} - \sigma(\Delta\kappa_V, \lambda_V)}{\Delta\sigma_{\text{SM}}} \right)^2, \tag{2}$$

where $\Delta\sigma_{\text{SM}} = \sigma_{\text{SM}} \sqrt{\delta_{\text{stat.}}^2}$ with $\delta_{\text{stat.}} = 1/\sqrt{N_{\text{SM}}}$ and $N_{\text{SM}} = \sigma_{\text{SM}} L$. In our calculations, we consider that two of the couplings ($\Delta\kappa, \lambda$) are assumed to deviate from their SM value. We estimate the sensitivity to the anomalous couplings at 95 C.L. at the LHeC for the integrated luminosities of 10 fb^{-1} and 100 fb^{-1} . The contour plots of anomalous couplings in $\Delta\kappa_\gamma - \lambda_\gamma$ plane for the integrated luminosities of 10 fb^{-1} and 100 fb^{-1} at electron beam energies $E_e = 60$ (140) GeV with different polarizations are given in Figs. 11–16. For

the process $ep \rightarrow \nu_e q ZX$, we make analysis of the signal and backgrounds when Z decays leptonically, $Z \rightarrow l^+l^-$, where $l = e, \mu$. The contour plots of anomalous couplings in $\Delta\kappa_Z - \lambda_Z$ plane for the integrated luminosities of 10 fb^{-1} and 100 fb^{-1} at electron beam energies of $E_e = 60(140) \text{ GeV}$ with different polarizations are presented in Figs. 17–22.

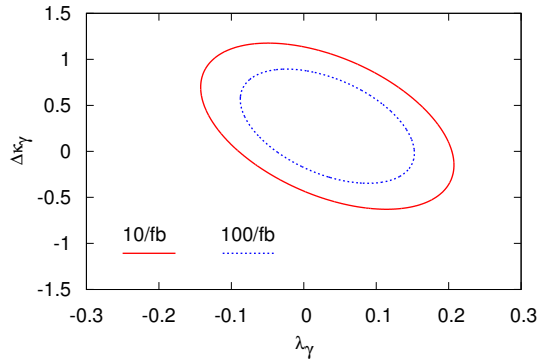


Fig. 11. Two dimensional 95% C.L. contour plot of anomalous couplings in the $\lambda_\gamma - \Delta\kappa_\gamma$ plane for the integrated luminosity of 10 fb^{-1} and 100 fb^{-1} at electron beam energy $E_e = 60 \text{ GeV}$ with the beam polarization $P_e = 0.8$.

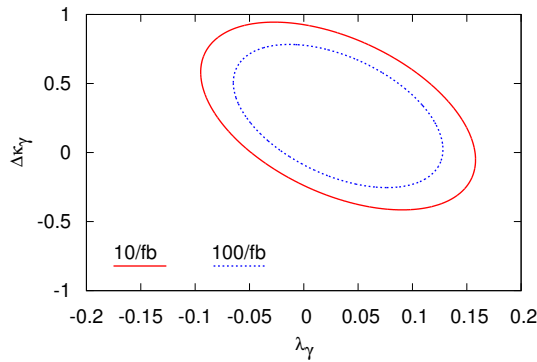


Fig. 12. The same as Fig. 11 but for $P_e = 0$.

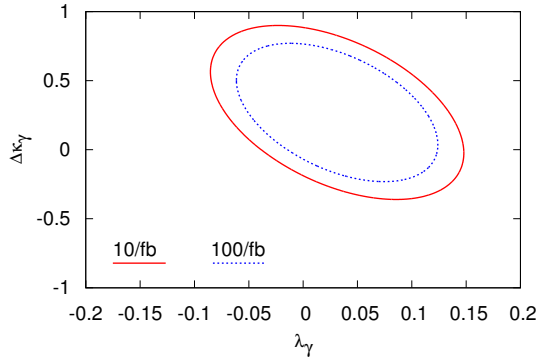


Fig. 13. The same as Fig. 11 but for $P_e = -0.8$.

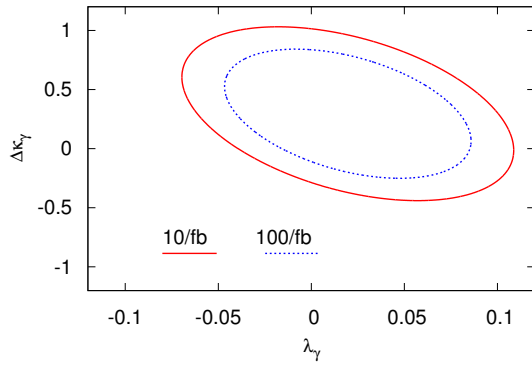


Fig. 14. Two dimensional 95% C.L. contour plot anomalous couplings in the λ_γ - $\Delta\kappa_\gamma$ plane for the integrated luminosity of 10 fb^{-1} and 100 fb^{-1} at electron beam energy $E_e = 140 \text{ GeV}$ with polarization $P_e = 0.8$.

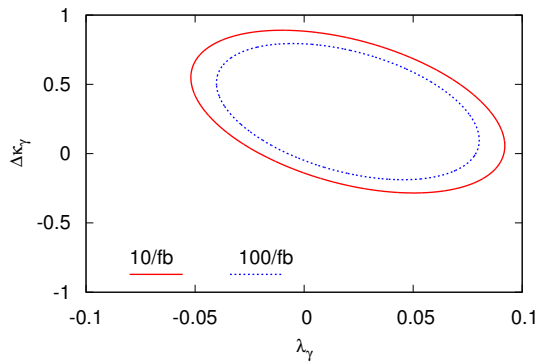


Fig. 15. The same as Fig. 14 but for $P_e = 0$.

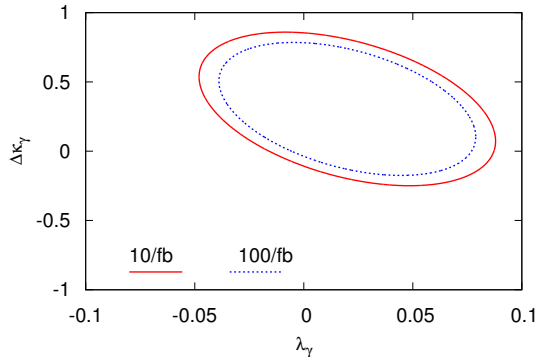


Fig. 16. The same as Fig. 14 but for $P_e = -0.8$ GeV.

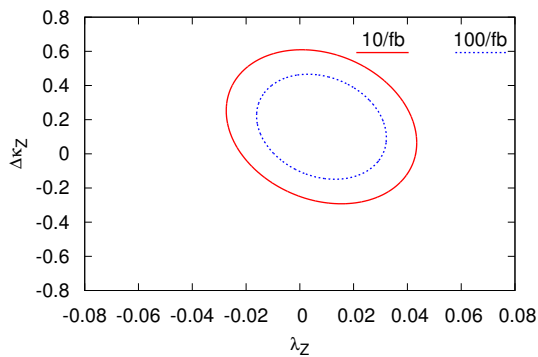


Fig. 17. Two dimensional 95% C.L. contour plot of anomalous couplings in the λ_Z - $\Delta\kappa_Z$ plane for the integrated luminosity of 10 fb^{-1} and 100 fb^{-1} at electron beam energy $E_e = 60$ GeV with polarization $P_e = 0.8$.

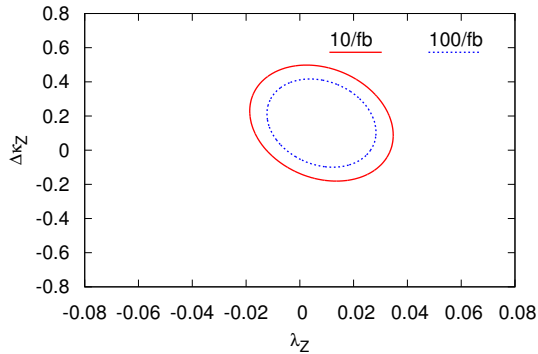


Fig. 18. The same as Fig. 17 but for $P_e = 0$.

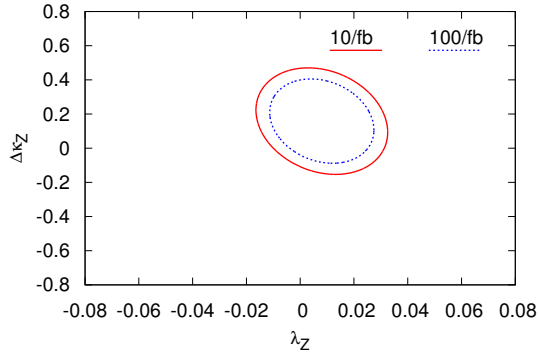


Fig. 19. The same as Fig. 17 but for $P_e = -0.8$.

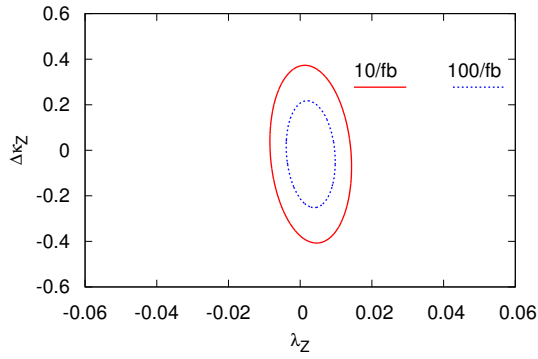


Fig. 20. Two-dimensional 95% C.L. contour plot of anomalous couplings in the λ_Z - $\Delta\kappa_Z$ plane for the integrated luminosity of 10 fb^{-1} and 100 fb^{-1} at electron beam energy $E_e = 140 \text{ GeV}$ with polarization $P_e = 0.8$.

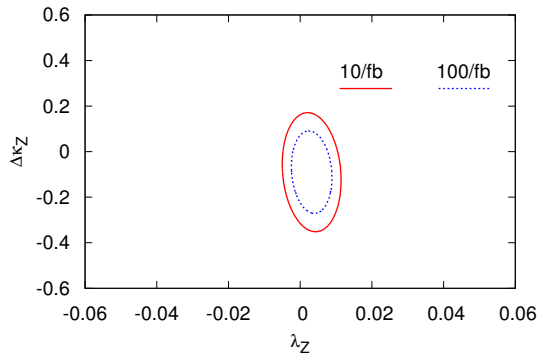


Fig. 21. The same as Fig. 20 but for $P_e = 0$.

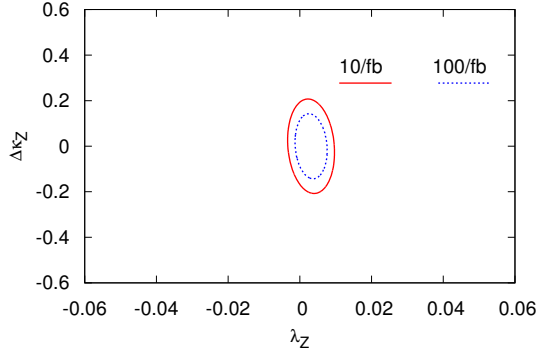


Fig. 22. The same as Fig. 20 but for $P_e = -0.8$.

The difference of the upper and lower bounds on the anomalous couplings $\Delta\kappa_V$ and λ_V (where $V = \gamma, Z$) can be written as

$$\delta\Delta\kappa_V = \Delta\kappa_V^{\text{upper}} - \Delta\kappa_V^{\text{lower}}, \quad \delta\lambda_V = \lambda_V^{\text{upper}} - \lambda_V^{\text{lower}}. \quad (3)$$

The current limits on anomalous couplings and the difference of the upper and lower bounds for electron beam energies of $E_e = 60$ and 140 GeV with integrated luminosities $L_{\text{int}} = 10 \text{ fb}^{-1}$ and 100 fb^{-1} at LHeC with the unpolarized (polarized) electron beam are given in Tables III–VI. We have obtained two-parameter limits on $\delta\Delta\kappa_\gamma$ and $\delta\lambda_\gamma$ which can be compared to the ATLAS and CMS results. However, the current limits on $\delta\lambda_Z$ is found to be much more sensitive at the LHeC.

TABLE III

The 95% C.L. current limits on the anomalous couplings and the difference of the upper and lower bounds for electron beam energy of $E_e = 60$ GeV with $L_{\text{int}} = 10 \text{ fb}^{-1}$ for polarized and unpolarized electron beam.

P_e	$\Delta\kappa_\gamma$	$\delta\Delta\kappa_\gamma$	λ_γ	$\delta\lambda_\gamma$
-0.8	[-0.366, 0.899]	1.265	[-0.085, 0.148]	0.233
0	[-0.421, 0.940]	1.361	[-0.094, 0.159]	0.253
0.8	[-0.641, 1.177]	1.818	[-0.141, 0.208]	0.349
P_e	$\Delta\kappa_Z$	$\delta\Delta\kappa_Z$	λ_Z	$\delta\lambda_Z$
-0.8	[-0.152, 0.471]	0.623	[-0.016, 0.033]	0.049
0	[-0.180, 0.498]	0.677	[-0.018, 0.035]	0.053
0.8	[-0.293, 0.611]	0.904	[-0.027, 0.044]	0.071

TABLE IV

The same as Table III but for $L_{\text{int}} = 100 \text{ fb}^{-1}$.

P_e	$\Delta\kappa_\gamma$	$\delta\Delta\kappa_\gamma$	λ_γ	$\delta\lambda_\gamma$
-0.8	[-0.237, 0.771]	1.008	[-0.061, 0.124]	0.185
0	[-0.257, 0.777]	1.034	[-0.064, 0.128]	0.192
0.8	[-0.356, 0.893]	1.249	[-0.087, 0.153]	0.240
P_e	$\Delta\kappa_Z$	$\delta\Delta\kappa_Z$	λ_Z	$\delta\lambda_Z$
-0.8	[-0.088, 0.405]	0.493	[-0.011, 0.027]	0.038
0	[-0.104, 0.412]	0.516	[-0.012, 0.028]	0.040
0.8	[-0.147, 0.465]	0.612	[-0.016, 0.032]	0.048

TABLE V

The 95% C.L. current limits on the anomalous couplings and the difference of the upper and lower bounds for electron beam energy of $E_e = 140 \text{ GeV}$ with $L_{\text{int}} = 10 \text{ fb}^{-1}$ for polarized and unpolarized electron beam.

P_e	$\Delta\kappa_\gamma$	$\delta\Delta\kappa_\gamma$	λ_γ	$\delta\lambda_\gamma$
-0.8	[-0.255, 0.865]	1.120	[-0.049, 0.088]	0.137
0	[-0.288, 0.895]	1.183	[-0.052, 0.092]	0.144
0.8	[-0.255, 1.035]	1.120	[-0.070, 0.109]	0.179
P_e	$\Delta\kappa_Z$	$\delta\Delta\kappa_Z$	λ_Z	$\delta\lambda_Z$
-0.8	[-0.208, 0.207]	0.415	[-0.003, 0.010]	0.013
0	[-0.350, 0.170]	0.520	[-0.005, 0.012]	0.017
0.8	[-0.407, 0.373]	0.780	[-0.008, 0.014]	0.022

TABLE VI

The same as Table V but for $L_{\text{int}} = 100 \text{ fb}^{-1}$.

P_e	$\Delta\kappa_\gamma$	$\delta\Delta\kappa_\gamma$	λ_γ	$\delta\lambda_\gamma$
-0.8	[-0.182, 0.793]	0.975	[-0.039, 0.079]	0.118
0	[-0.192, 0.798]	0.990	[-0.041, 0.081]	0.122
0.8	[-0.251, 0.844]	1.095	[-0.047, 0.086]	0.133
P_e	$\Delta\kappa_Z$	$\delta\Delta\kappa_Z$	λ_Z	$\delta\lambda_Z$
-0.8	[-0.143, 0.142]	0.285	[-0.001, 0.008]	0.009
0	[-0.273, 0.089]	0.362	[-0.003, 0.009]	0.012
0.8	[-0.253, 0.215]	0.468	[-0.004, 0.010]	0.014

5. Conclusions

The $WW\gamma$ and WWZ anomalous interactions through the processes $ep \rightarrow \nu_e q \gamma X$ and $ep \rightarrow \nu_e q Z X$ can be studied independently at the LHeC. We obtain two-parameter accessible ranges of triple gauge boson anomalous couplings at the LHeC with the polarized and unpolarized beam at the energies of $E_e = 60$ GeV and $E_e = 140$ GeV. Our limits compare with the results from two-parameter analysis given by ATLAS and CMS collaborations [7, 8]. We find that the sensitivities to anomalous couplings $\Delta\kappa_V$ ($V = \gamma, Z$) will be of the order of 10^{-1} , which is an order of magnitude larger than the SM loop level sensitivity of 10^{-2} , however a measurement of these couplings above 10^{-2} would offer a possible new physics signal. We conclude that the anomalous coupling λ_Z can be best constrained with the sensitivity of the order of 10^{-3} at the LHeC with polarized electron beam. The LHeC will give complementary information about anomalous couplings compared to Tevatron and the LHC.

The work of O.C. is partially supported by the State Planning Organisation (DPT) — the Ministry of Development under grant No. DPT2006K-120470. A.S. would like to thank the Abant Izzet Baysal University Department of Physics, where a part this study was carried out, for their hospitality.

REFERENCES

- [1] U. Baur, D. Zeppenfeld, *Nucl. Phys.* **B325**, 253 (1989); C.S. Kim, W.J. Stirling, *Z. Phys.* **C53**, 601 (1992); S. Atag, I.T. Cakir, *Phys. Rev.* **D63**, 033004 (2001).
- [2] C.B. Mariotto, M.V.T. Machado, *Phys. Rev.* **D86**, 033009 (2012).
- [3] S.S. Biswal, M. Patra, S. Raychaudhuri, [arXiv:1405.6056](https://arxiv.org/abs/1405.6056) [hep-ph].
- [4] S. Schael *et al.* [ALEPH, DELPHI, L3, OPAL and LEP Electroweak collaborations], *Phys. Rep.* **532**, 119 (2013).
- [5] T. Aaltonen *et al.* [CDF Collaboration], *Phys. Rev.* **D76**, 111103(R) (2007); *Phys. Rev. Lett.* **104**, 201801 (2010).
- [6] V.M. Abazov *et al.* [D0 Collaboration], *Phys. Lett.* **B718**, 451 (2012).
- [7] ATLAS Collaboration, *Phys. Rev.* **D87**, 112001 (2013); **D87**, 112003 (2013).
- [8] CMS Collaboration, *Eur. Phys. J.* **C73**, 2610 (2013); *Phys. Rev.* **D89**, 092005 (2014).
- [9] J.L. Abelleira Fernandez *et al.* [LHeC Study Group], *J. Phys. G* **39**, 075001 (2012) [[arXiv:1206.2913](https://arxiv.org/abs/1206.2913) [physics.acc-ph]].
- [10] K. Hagiwara, R. Peccei, D. Zeppenfeld, K. Hikasa, *Nucl. Phys.* **B282**, 253 (1987).

- [11] E.N. Argyres *et al.*, *Nucl. Phys.* **B391**, 23 (1993); P. Kalyniak *et al.*, *Phys. Rev.* **D48**, 5081 (1993); G. Couture *et al.*, *Phys. Rev.* **D36**, 859 (1987).
- [12] A. Belyaev, N. Christensen, A. Pukhov, *Comput. Phys. Commun.* **184**, 1729 (2013); arXiv:1207.6082 [hep-ph].
- [13] J. Pumplin *et al.*, *J. High Energy Phys.* **0207**, 012 (2002) [arXiv:hep-ph/0201195].